Progress Report on Work Performed on the LIBRA Design During the Period 1 February 1987 to 31 January 1988

B. Badger, G. Kulcinski, G. Moses, E. Lovell, R. Engelstad, J. MacFarlane, Z. Musicki, R. Peterson, M. Sawan, I. Sviatoslavsky, and L. Wittenberg

January 1988

FPA-88-1

FUSION POWER ASSOCIATES

2 Professional Drive, Suite 248
Gaithersburg, Maryland 20879
(301) 258-0545

1500 Engineering Drive
Madison, Wisconsin 53706
(608) 263-2308

PROGRESS REPORT ON WORK PERFORMED ON THE LIBRA DESIGN DURING THE PERIOD 1 FEBRUARY 1987 to 31 JANUARY 1988

B. Badger, G. Moses, R. Engelstad, G. Kulcinski, E. Lovell, J. MacFarlane, Z. Musicki, R. Peterson, M. Sawan, I. Sviatoslavsky, L. Wittenberg

Fusion Power Associates
6515 Grand Teton Plaza
Madison, WI 53719

January 1988

FPA-88-1

TABLE OF CONTENTS

1. INTRODUCTION

The first year's activity on the LIBRA project has been completed. This project is a joint effort between KfK, Fusion Power Associates (FPA), Sandia National Laboratory (SNL), Pulse Sciences Incorporated (PSI) and the University of Wisconsin (UW). The main goal is to provide a preconceptual design for a light ion beam driven commercial power plant. It is anticipated that the first public presentation of this design will be at the Beams-88 meeting in Karlsruhe in July of 1988. After peer review of the concept, a final report will be completed by the end of 1988.

The division of responsibilities for the work has left FPA with the following responsibilities:

Plasma Channel Formation
Target Injection (with KfK)
Neutronics
Blanket and Shield Design
Design Integration

The main effort in 1987 has focussed on the first 4 and it is anticipated a major effort on item 5 (Design Integration) will be made in 1988.

Other areas such as the diode design and driver technology have also occupied much of the effort by the other participants in 1987. A workshop on repetitive diodes was held at Sandia National Laboratory on July 8, 1987 and a report of that meeting has been issued. Another meeting on driver development was held in Madison, WI on November 9, 1987 and a report of that activity is in progress.

This progress report contains brief descriptions of some of the key work conducted in 1987 by FPA alone. More detail on this work is given in the proceedings of previous design meetings held in Madison on May 19-20, 1987 and November 12, 1987. The reader is referred to these proceedings as a supplement to this brief summary.

2. CHANNEL FORMATION

Channel formation is a very important issue for the LIBRA conceptual design and for light ion fusion in general. LIBRA requires plasma discharge channels to propagate the ion beams from the ion diodes to the target. The parameters for the LIBRA channels are shown in Table 2-1. The most important features of this channel design are the channel length, the channel radius, and the required magnetic field at the channel radius. An attempt has been made to design a channel for LIBRA that can provide this 28 kG field at a point 0.5 cm from the channel axis. In this effort, we have used the ZPINCH computer code to simulate the radial behavior of the plasma channels.[1]

Table 2-1. LIBRA Channel Parameters

Channel Length	5.4 m
Channel Radius	.5 cm
Target Chamber Gas	3.55×10^{17} cm^{-3} Ar + 0.2% Li
Average Beam Ion Energy	30 MeV
Maximum Injection Angle into Channel	0.15 radians
Ion Species	Li^3
Ion Power Injected Into Channel	9.5 TW
Power Bunching in Channel	4.4
Ion Power on Target per Channel	25 TW
Ion Energy Loss in Channel	25%
Fraction of Ions Reaching Target	80%
Number of Main Pulse Beams	16
Number of Prepulse Beams	2
Number of Channels	36
Maximum Discharge Current	100 kA
Discharge Current Shape	Double Pulse
Required Magnetic Field at Channel Radius	28 kG

We have designed a channel that provides a magnetic field 0.5 cm from the channel axis that may be as high as 20 kG, still less than the required 28 kG but more than the roughly 8 kG that we could achieve at the beginning of this study. To achieve this field

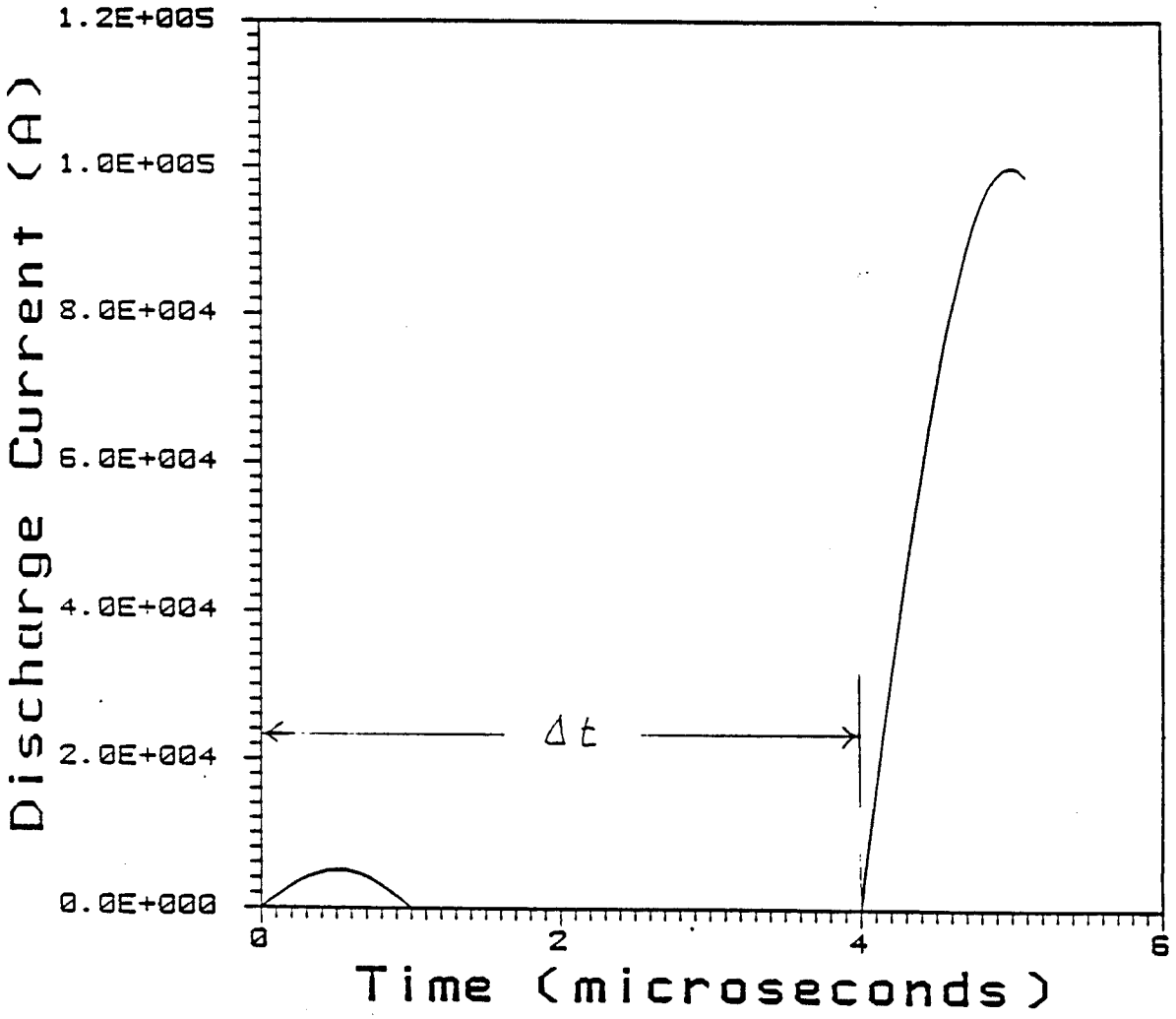

Figure 2-1. Discharge Current History for LIBRA Channels.

we have used a discharge current history of the type shown in Fig. 2-1, where a large pulse follows a smaller one. For the calculation presented here, the time delay of the second pulse, Δt, is 1 μs. We have also found that a better channel is formed if the radius of the pre-ionizing laser is 0.2 cm[2] and have used this value for these calculations. The magnetic field is plotted as a function of radius for various times in Fig. 2-2. One can see that at a radius of 0.5 cm, the magnetic field is roughly 20 kG.

In the above channel calculation, we have neglected the effects of radiant heat transfer. The radiation diffusion model currently used in ZPINCH predicts that radiative heat transfer plays a dominant roll. We have reason to believe, however, that for physically small systems the radiation diffusion method predicts radiant heat fluxes that are too high. This has been noticed when we have compared similar computer simulations with other small experiments.[3] If this is the case for channel calculations, the true result will be neither the calculations with radiation nor those without, but will be somewhere in between. Experiment will tell where in this range the correct values lie.

It is planned to improve the physical models used in ZPINCH to model radiant heat transfer. With this improved version of the code, we will continue to work to increase the magnetic fields in the channels.

References for Section 2

1. J.J. Watrous, G.A. Moses, and R.R. Peterson, "Z-PINCH - A Multifrequency Radiative Transfer Magnetohydrodynamics Computer Code," University of Wisconsin Fusion Technology Institute Report UWFDM-584 (June 1987).

2. B. Badger et al., "Light Ion Beam Fusion Target Development Facility Studies: Progress Report for the Period 1 November 1986 to 30 October 1987," University of Wisconsin Fusion Technology Institute Report UWFDM-752 (January 1987).

3. J.J. MacFarlane, G.A. Moses, and R.R. Peterson, "Energy Deposition and Shock Wave Evolution from Laser-Generated Plasma Expansions," University of Wisconsin Fusion Technology Institute Report UWDFM-723 (May 1987).

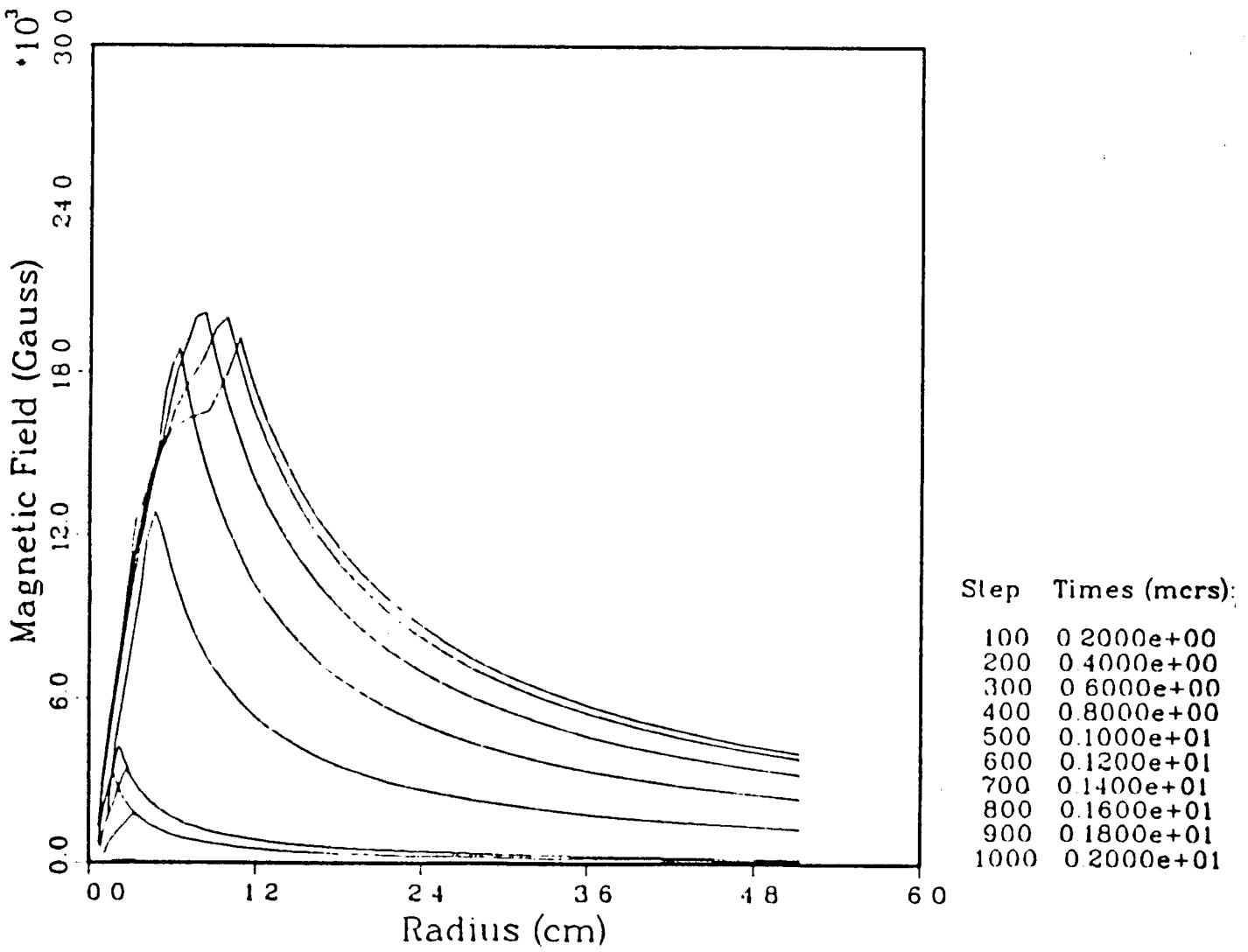

Figure 2-2. Magnetic Field Profiles in LIBRA Channels with No Radiation Transport.

3. TARGET HEATING DURING INJECTION

The LIBRA target design requires that the DT fuel must be at solid or liquid density and in a very symmetric hollow spherical shell at the time of target irradiation by the light ion beams. Before the target injection, the whole target is cooled to 4 K, but the target is subjected to various heat loads during injection that can heat the DT fuel. We have considered the fuel temperature limits, the heat loads during injection, and have calculated the temperature profiles in the target as a function of time.

The limits on the DT fuel in a cryogenic target depend, to some degree, on the target design. If the fuel is pure frozen DT, then the fuel must not melt, so the temperature must be below the triple point of 19.7 K. Also, the vapor density in the hollow void, which is a strong function of the fuel temperature, is dictated by target design. In HIBALL,[1] we took this temperature limit to be 14 K, but this was rather arbitrary and a higher fuel temperature might be acceptable. Another option that has recently come to light[2] is the use of a very low density, but very rigid, foam to hold liquid DT in a spherical shell. Because the fuel can be liquid, the fuel temperature can be above the triple point for DT, but it is still limited by the vapor density criterion. Some work predicts that the fuel temperature in such a target could be as high as 30 K.

We have considered three heat loads to the cryogenic target: friction in the gun barrel of the pneumatic target injector, radiant heat from the target chamber, and convective heat from the target chamber gas. While the target is in the gun barrel, it is in a teflon sabot that should protect it from the friction with the barrel. We have used the same sabot design as in HIBALL and have used a frictional heating of 51 W/cm^2. When the target leaves the barrel, our calculations show that only the sabot has been heated and the target is still at 4 K. When the target is moving through the 800 K argon gas in the target chamber at 200 m/s, it experiences a 3.5 W/cm^2 convective heat load and a 2 W/cm^2 radiant heat load. Using a finite-difference heat transfer computer code with temperature dependent thermal properties and the target design shown in Fig. 3-1, we have calculated the temperature profiles in the target at various times. These are shown in Fig. 3-2. Here, one can see that at 25 ms after the target is injected into the target chamber (the time that it reaches the center), the outer edge of the fuel is slightly above 20 K. For this reason, we recommend that the target use the foam concept to keep this molten portion of the fuel in a spherical shape. The heating of the target could be reduced by lowering the gas temperature or by increasing the target injection velocity.

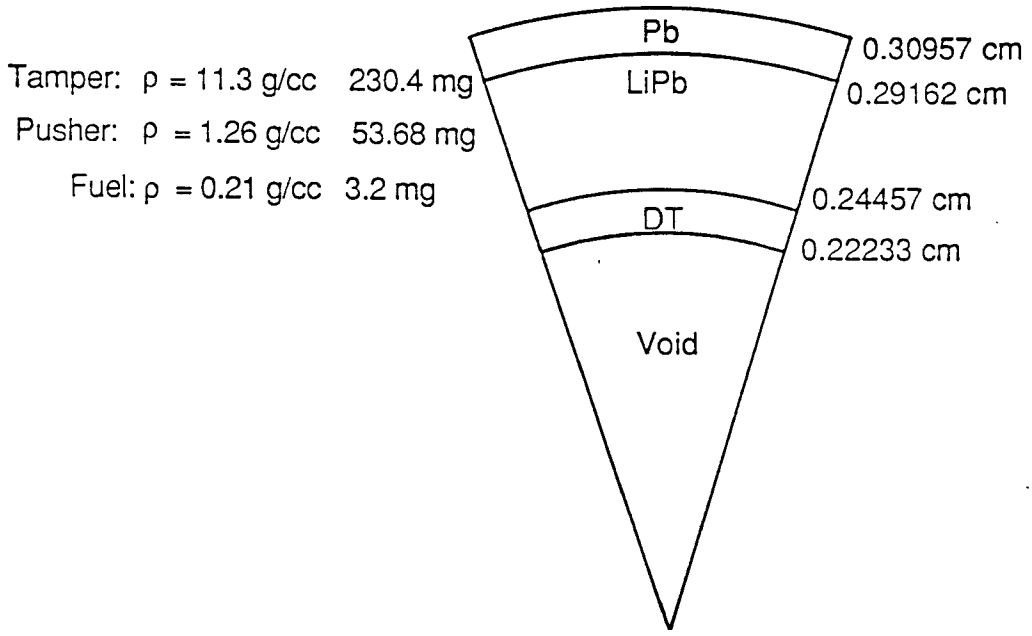

Figure 3-1. Current LIBRA Target Design.

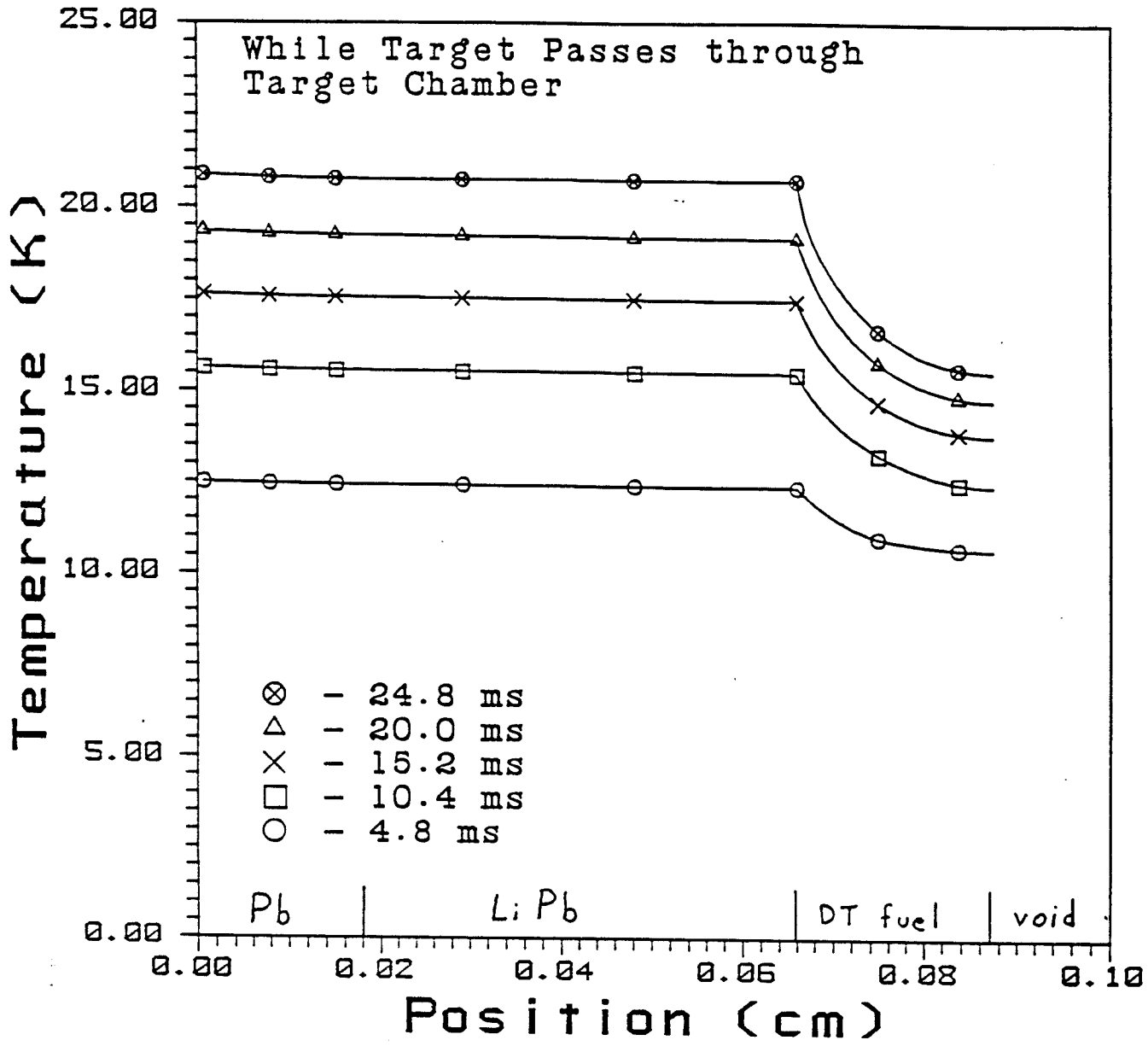

Figure 3-2. Temperature Profiles in LIBRA Target After Injection into Target Chamber.

Increasing the velocity would increase the convective heating rate by the velocity to the 0.6 power, so the second option would only slowly decrease the fuel temperature.

References for Section 3

1. B. Badger et al., "HIBALL-II - An Improved Conceptual Heavy Ion Beam Driven Fusion Reactor Study," Kernforschungszentrum Karlsruhe Report KfK-3840 (December 1984).

2. R.A. Sacks and D.H. Darling, "Direct Drive Cryogenic ICF Capsules Employing D-T Wetted Foam," Nuclear Fusion 27, 447 (1987).

4. CAVITY CLEARING

The behavior of the target chamber gas in LIBRA has been studied after the explosion of the 320 MJ target. The target yield is partitioned into 231 MJ of neutrons, 63 MJ into x-rays, and 26 MJ into target debris ions. The argon target chamber gas is assumed to be at a density of 3.55×10^{17} cm^{-3}. In the LIBRA target chamber, the first row of INPORT tubes forms a cylinder 3 meters in radius. We have approximated the target chamber by a sphere 3 meters in radius and have analyzed the gas behavior with the CONRAD computer code.[1] It was found that, of the original 63 MJ in x-rays, only 6 MJ reach the three meter radius that we have taken as the position of the tubes. This 6 MJ vaporizes 2.9 kg of LiPb from the tubes. The sum of the recoil impulse and the shock impulse is about 100 Pa-s. In the first few ms after the target explosion, about 60 MJ are radiated to the tubes by the gas, leaving about 20 MJ in the gas. This leads to an average pressure in the gas of about 290 torr and an average gas temperature of about 9000 K. Radiation cannot reduce the pressure and temperature very much in the next 0.3 s before the next shot, so we must find another way of recovering this 20 MJ.

General Description

The vacuum system for LIBRA is based on steady state pumping by roots blowers backed up by conventional dry sealed roughing pumps. Such a design requires a buffer tank which we call the suppression chamber which has a triple function:

1. To extract energy from the evacuated gas to be used in the power cycle.
2. To act as a buffer for smoothing out the pressure fluctuation during reactor operation.
3. To condense any mist that may exist with the evacuated gas.

The suppression chamber has LiPb in the bottom of it and exhaust pipes from the target chamber are submerged just below the liquid level as shown in the schematic of Fig. 4-1. The temperature of the LiPb in the suppression chamber is maintained at 350°C (623 K) and the pressure is the same as that in the target chamber, 26 torr. The temperature of the gas in the target chamber just prior to a shot is 800 K and thus the 26 torr is equivalent to a pressure of 10 torr at 300 K. Immediately after the shot, the pressure in the target chamber reaches 290 torr and the temperature 9000 K. This high pressure will cause the gas from the target chamber to be forced through the exhaust pipes into the suppression chamber until the pressure in both chambers equilibrates. At equilibration, the temperature in the target chamber will be higher than the temperature before

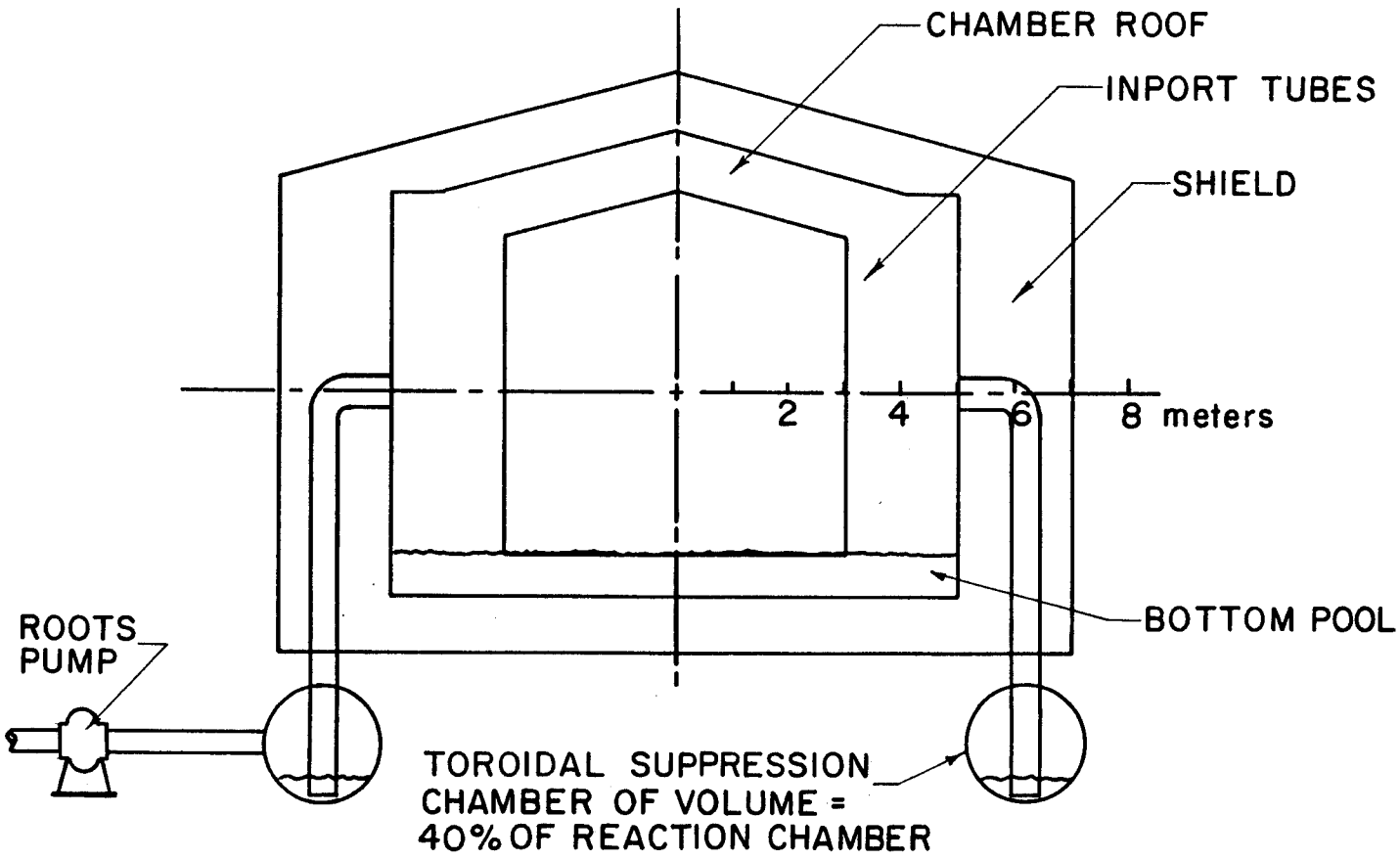

Figure 4-1. Schematic Cross Section of LIBRA Chamber with a Suppression Chamber Shown to Scale for $V_s/V_t = 0.4$.

the shot. The liquid level in the suppression chamber will prevent any further gas exhaust, and as the temperature of the gas in the target chamber cools down to the initial 800 K, the pressure falls below 26 torr.

To cool the gas in the suppression chamber to 623 K, it may be necessary to disperse LiPb to provide the needed large surface area for heat exchange. This will also condense any vapor or mist that may still be present in the gas. Bubbling the gas through the LiPb pool in the suppression chamber also will cool it. From the suppression chamber, the gas is pumped by roots blowers backed by dry sealed roughing pumps. The LiPb from the suppression chamber is then recycled back to the target chamber.

Procedure for Calculating Pumping Requirement

Table 4-1 gives the parameters used to calculate the pumping requirements. The needed capacity of the vacuum pumping system depends on the size of the suppression chamber and the temperature of the gas in it. It also depends on the temperature of the gas in the target chamber at the time the pressures equilibrate in the target and suppression chambers.

Precise determination of the temperature in the LIBRA chamber upon pressure equilibration is very difficult. In the present calculation we make the following conservative assumptions:

- The gas in the target chamber after the shot undergoes an isentropic expansion into the suppression chamber.
- The gas remaining in the INPORT tube zone is assumed to cool to the maximum temperature of the tubes, 773 K (500°C).
- The gas in the center of the target chamber (not in the INPORT tube zone) remains at the temperature reached during the isentropic expansion.
- The temperature of the gas is then averaged for these two zones and the pressure in the target chamber is then based on this average temperature.

The volume of the suppression chamber is varied from $\frac{V_s}{V_t}$ of 0.1 - 1.0. Table 4-2 gives the calculated results for this range of chambers volume ratios. It gives the isentropic expansion temperature, the average temperature and the gas pressure upon equilibration of pressures between the suppression and the target chambers. It also gives the pressure ratio of the equilibrated pressure to the final pumpdown pressure. This is the sudden pressure fluctuation that the roots blowers must deal with and must not exceed a value of 2.0. This eliminates the range of $\frac{V_s}{V_t} < 0.4$. The table also gives the fraction of the gas in the target chamber evacuated per shot. Finally the pumping speed

Table 4-1.

General Parameters Used to Calculate Required Pumping Speed

Radius to INPORT tubes (m)	3.0
Radius to Vacuum Wall (m)	5.0
Height from Bottom Pool to Roof (m)	6.0
Volume Fraction in INPORT Zone (%)	33
Gas in Chamber	Argon
Volume of Gas in INPORT Zone (m^3)	202
Volume of Gas in Cavity Center (m^3)	170
Pressure in Chamber Before Shot (torr)	26
Temperature in Chamber Before Shot (K)	800
Pressure in Chamber After Shot (torr)	290
Temperature in Chamber After Shot (K)	9000

Table 4-2.

Pumping Parameters for LIBRA

Ratio of Suppression Chamber Volume to Target Chamber Volume	Gas Temperature In Target Chamber After Isentropic Expansion (K)	Gas Average Temperature in Target Chamber After Equilibrium with Suppression Chamber (K)	Gas Average Pressure in Target Chamber and Suppression Chamber After Equilibrium (torr)	Ratio of Pressure After Equilibrium to Steady State Pressure	Fraction of Target Chamber Gas Mass Exhausted per Shot (%)	Pumping Speed Required (l/s)
1.0	1440	1076	29	1.12	16.4	1.23×10^5
0.8	1652	1173	30.8	1.47	19.3	1.53×10^5
0.5	2193	1420	35.2	1.76	23.4	1.80×10^5
0.4	2496	1557	38.2	1.95	24.4	1.78×10^5
0.3	2955	1767	42.9	2.21	25.3	1.70×10^5
0.2	3628	2052	50.3	2.57	24.4	1.47×10^5
0.1	4950	2647	68	2.60	21	1.08×10^5

required is given assuming a rep rate of 3 Hz. Figure 4-2 shows the pumping speed required as a function of the $\frac{V_s}{V_t}$ ratio. The useful range is $\frac{V_s}{V_t} > 0.4$ for which the pressure ratio is less than 2.0. The effective pumping speed falls in the range of 1.23×10^5 l/s to 1.78×10^5 l/s.

The most cost effective system must trade the cost of the suppression chamber with the price of the added pumping speed. It would seem that the price of the larger suppression chamber would be low compared to a ~ 50% higher pumping requirement and thus the choice would be toward the higher values of $\frac{V_s}{V_t}$. Further, because the pressure ratio is lower for the large suppression chamber, the roots blower can handle it more easily.

Reference for Section 4

1. R.R. Peterson "CONRAD - A Combined Hydrodynamics-Condensation/Vaporization Computer Code," University of Wisconsin Fusion Technology Institute Report UWFDM-670 (April 1986).

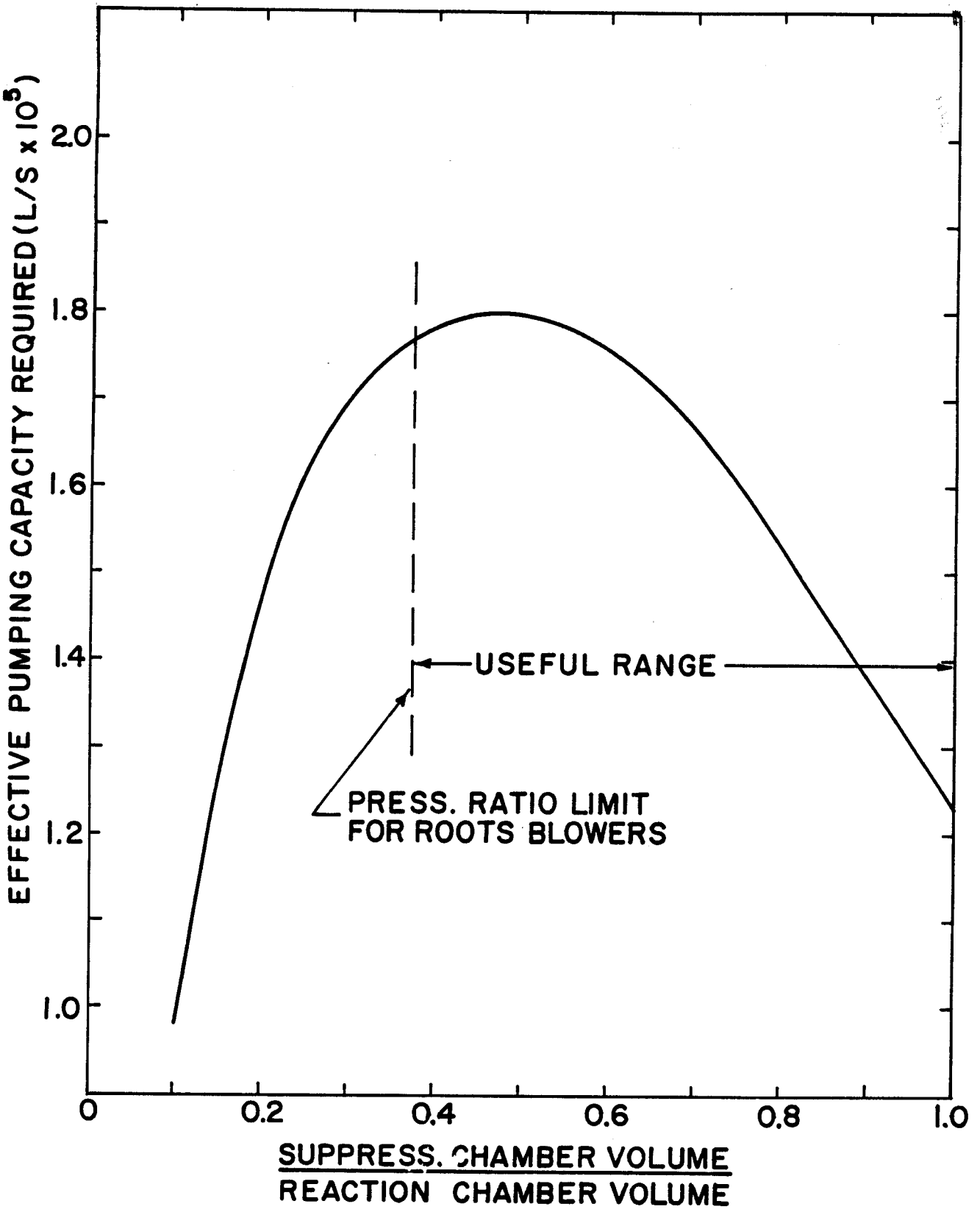

Figure 4-2. Effective Pumping Requirement for LIBRA as a Function of Suppression Chamber Volume.

5. NEUTRONICS

Neutronics Benchmark Calculations

One-dimensional neutronics calculations have been performed by FPA using the ONEDANT discrete ordinates code, the P_3-S_8 transport approximation and spherical geometry. The calculations were performed for ten different cases with different blanket thicknesses (Δ_B), different reflector thicknesses (Δ_r) and different lithium enrichments (% ^{6}Li). In all cases a point neutron source emitting neutrons with the HIBALL spectrum was used. The cavity radius is 3 m and a 1 m thick water shield was used at the back of the reflector to properly represent the boundary condition. The blanket consists of INPORT tubes with 0.33 packing fraction. The tubes consist of 2 vol% SiC and 98 vol% $Li_{17}Pb_{83}$. The reflector consists of 90 vol% HT-9 and 10 vol% $Li_{17}Pb_{83}$. The ONEDANT calculations have been performed using a 30 neutron - 12 gamma group cross section library based on the ENDF/B-V evaluation. Table 5-1 gives the ONEDANT results for the ten cases considered.

Tritium breeding ratio calculations have been performed by KfK for cases 2, 4, 6, 8, and 10 using the MCNP version 3 code and different MCNP continuous energy cross section libraries available to KfK. The geometrical model, nuclide densities and target spectrum used are identical to those used in the ONEDANT calculations performed by FPA. Analog Monte Carlo was used with no variance reduction method. Table 5-2 gives a comparison between the ONEDANT and MCNP results for tritium breeding ratio (TBR). These values take into account a target neutron multiplication of 1.046. The differences between the TBR values calculated by FPA and KfK are attributed to:

- Different calculational methods (discrete ordinates vs. Monte Carlo).
- Different energy treatments of cross sections (multigroup vs. continuous).
- Different cross section data (ENDF/B-V vs. ENDF/B-IV or ENDL85).

It is concluded from this analysis that excellent agreement with less than a 2% difference in TBR is obtained between the ONEDANT results using ENDF/B-V data and the MCNP results using the most recent ENDL85 data.

LIBRA Target Neutronics

Neutronics calculations have been performed for the LIBRA target using the one-dimensional discrete ordinates code ONEDANT. The target has 3.2 mg of DT that is compressed to a ρR value of 2 g/cm^2 at ignition. The target configuration at ignition used in the calculations is given in Fig. 5-1. The calculations were performed using spherical geometry and 30 neutron - 12 gamma group cross section data based on the

Table 5-1.

Nuclear Parameters Calculated by FPA for the 10 Cases

Case	Δ_B (m)	Δ_r (m)	%^{6}Li	TBR	M_n	M^*_o	Peak HT-9 dpa/FPY
1	2	.5	7.42	1.152	1.366	1.250	2.44
2	2	.5	90	1.625	1.259	1.174	1.21
3	1.5	.5	7.42	0.957	1.407	1.280	5.37
4	1.5	.5	90	1.659	1.278	1.189	3.12
5	1.0	.5	7.42	0.715	1.451	1.312	11.63
6	1.0	.5	90	1.406	1.293	1.200	7.95
7	1.0	.5	35	1.168	1.346	1.237	9.89
8	0.55	.5	90	1.162	1.309	1.211	18.00
9	1.0	.8	35	1.175	1.377	1.258	9.71
10	0.55	0.85	90	1.177	1.374	1.238	17.61

Table 5-2.

Comparison Between TBR Results Obtained by FPA and KfK

Case	FPA ONEDANT Results	KfK MCNP Results 23 July 87	1 Nov. 87	12 Nov. 87
2	1.625	1.659	1.670	—
4	1.549	1.580	1.591	1.570
6	1.406	1.427	1.442	1.409
8	1.162	1.159	1.193	1.138
10	1.177	1.245	1.254	1.173
Comments	Used as reference for comparison.	Results agree to within 2% except for case 10 the difference is 5.5%. This appears to be due to an overestimate of T_2 production in the reflector (27% higher than case 8).	Used ENDF/B-IV except for ^{6}Li, ^{12}C, and Si. Results agree to within 2.7% except for case 10 the difference is 6.5%.	Used ENDL85 except for ^{6}Li and ^{7}Li. All results agree to within 2%.

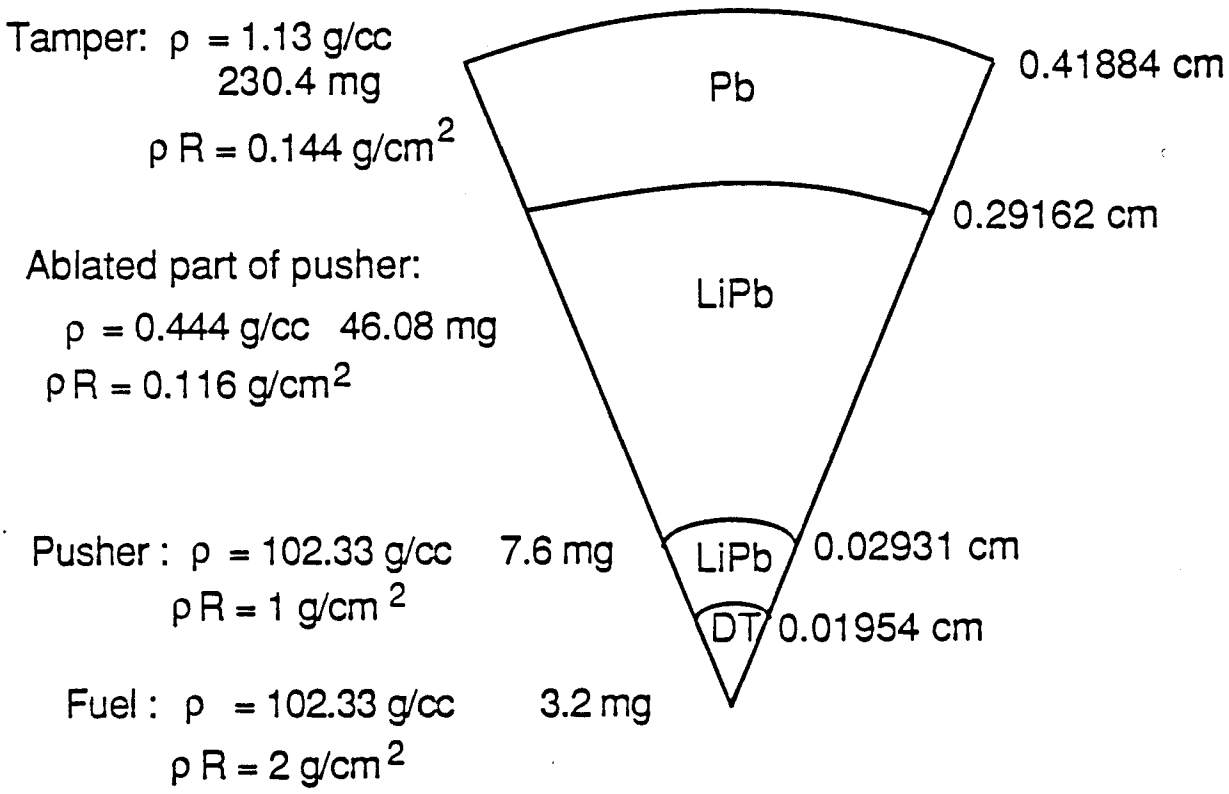

Figure 5-1. LIBRA Target Configuration at Ignition.

ENDF/B-V evaluation. A uniform 14.1 MeV neutron source was used in the compressed DT fuel zone.

The total energy deposited by neutrons and gamma photons in the target was calculated to be 1.377 MeV per DT fusion. Only 0.13% of this energy is deposited by gamma photons. About 87% of the energy is deposited in the DT fuel zone. Due to (n,2n) and (n,3n) reactions occurring in the target, 1.03 neutrons are emitted from the target for each DT fusion reaction. These neutrons carry an energy of 12.42 MeV implying that the average energy of neutrons emitted from the target is 12.07 MeV. For each DT fusion reaction, 0.017 gamma photons are emitted from the target with an average energy of 1.4 MeV. The energy spectra of neutrons and gamma photons emitted from the LIBRA target are shown in Fig. 5-2. Performing an energy balance for the target indicates that 0.28 MeV of energy is lost in endoergic reactions per DT fusion. For the LIBRA DT fuel yield of 320 MJ, the target yield was calculated to be 314.89 MJ. The neutron and gamma yields are 225.78 and 0.44 MJ, respectively, while the combined X-ray and debris yield is 88.67 MJ. The energy flow for the LIBRA target is given in Fig. 5-3.

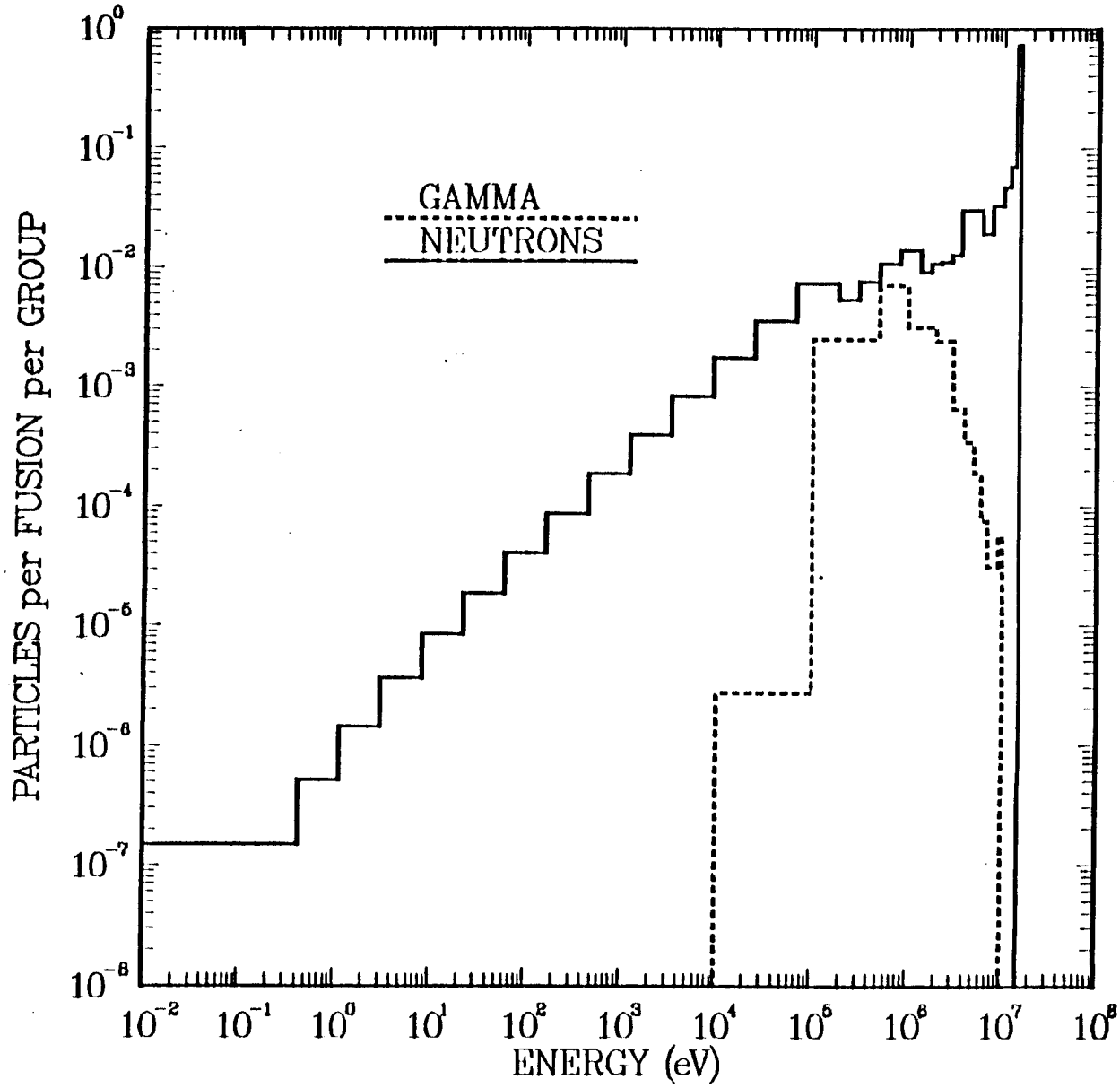

Figure 5-2. Energy Spectra of Neutrons and Gamma Photons Emitted from the LIBRA Target.

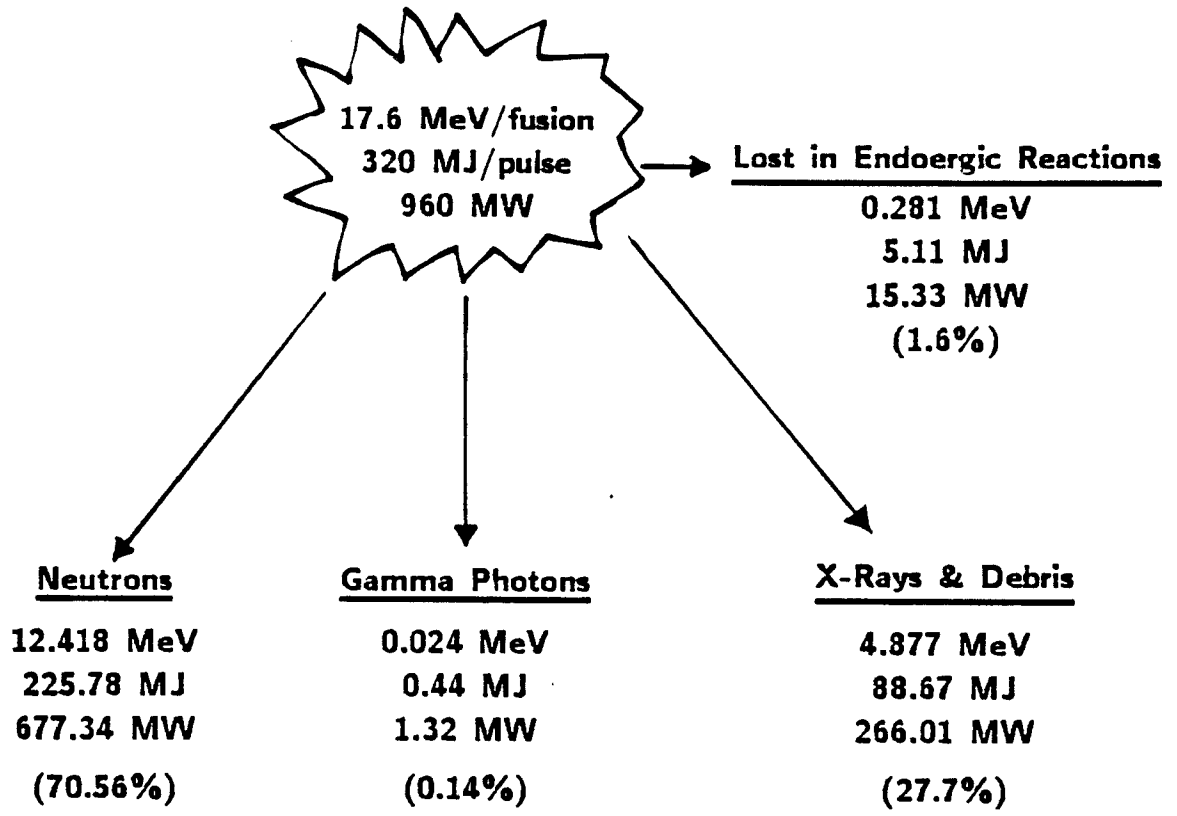

Figure 5-3. Energy Flow for LIBRA Target.

6. CHAMBER DESIGN

Chamber Neutronics Analysis

A one-dimensional scoping analysis was performed to determine the blanket design options that satisfy the tritium breeding and wall protection requirements. The ONEDANT code was used with the chamber modeled in one-dimensional spherical geometry. Multigroup cross section data based on ENDF/B-V were used in the calculations. A point source emitting neutrons and gamma photons with the spectra calculated for the LIBRA target was used at the center of the 3 m radius cavity. The results were normalized to a DT yield of 320 MJ and a repetition rate of 3 Hz. The blanket is made of banks of INPORT tubes with 0.33 packing fraction. The tubes consist of 2 vol% SiC and 98 vol% $Li_{17}Pb_{83}$. A 0.5 m thick reflector consisting of 90 vol% HT-9 and 10 vol% $Li_{17}Pb_{83}$ is used behind the blanket.

A minimum tritium breeding ratio (TBR) of 1.1 is required to achieve tritium self-sufficiency. In addition, the INPORT tubes are required to protect the first metallic wall. The peak end-of-life dpa in HT-9 is required to not exceed 200 dpa implying that for 30 FPY reactor life the peak dpa rate should not exceed 6.6 dpa/FPY. The design should also aim at maximizing the energy multiplication (M) due to its impact on the cost of electricity. In addition, the blanket thickness needs to be minimized to minimize the length of the channel used for beam propagation.

The calculations were performed for 12 cases with different blanket thicknesses (Δ_B) and lithium enrichments (% ^6Li). The results are given in Table 6-1. M_n is the nuclear energy multiplication in the blanket and reflector, while M_o is the overall energy multiplication that gives the ratio between the total energy deposited in the blanket and reflector and the DT yield. For a fixed lithium enrichment, increasing the blanket thickness results in increasing TBR, decreasing M and decreasing damage rate. Increasing the lithium enrichment for a given blanket thickness results in increasing TBR, decreasing M, and decreasing the dpa rate. The TBR and dpa rate values obtained for the different cases analyzed are mapped in Fig. 6-1. In order to satisfy the tritium breeding and wall protection requirements, the design point should be in the box indicated in the upper left corner of the graph. In order to satisfy the other design goals of minimizing the blanket thickness and maximizing M, it is clear that the design point should be at the right or lower boundaries of the box.

Table 6-1.

Neutronics Results for the Different Blanket Designs Considered in the Scoping Analysis

Case	$\%^6Li$	Δ_B (cm)	TBR	M_n	M_o	Peak dpa/FPY in HT-9	Peak He appm/FPY in HT-9
1	7.42	50	0.421	1.465	1.313	38.87	75.46
2	7.42	100	0.705	1.450	1.302	18.40	12.91
3	7.42	150	0.944	1.408	1.273	8.51	2.16
4	7.42	200	1.136	1.366	1.243	3.88	0.37
5	30	50	0.791	1.381	1.253	36.00	75.39
6	30	100	1.108	1.357	1.236	16.07	12.89
7	30	150	1.312	1.323	1.212	6.99	2.15
8	30	200	1.445	1.296	1.193	3.00	0.36
9	90	50	1.108	1.311	1.204	31.16	75.18
10	90	100	1.387	1.294	1.192	12.60	13.57
11	90	150	1.528	1.274	1.178	4.95	2.14
12	90	200	1.603	1.260	1.168	1.92	0.36

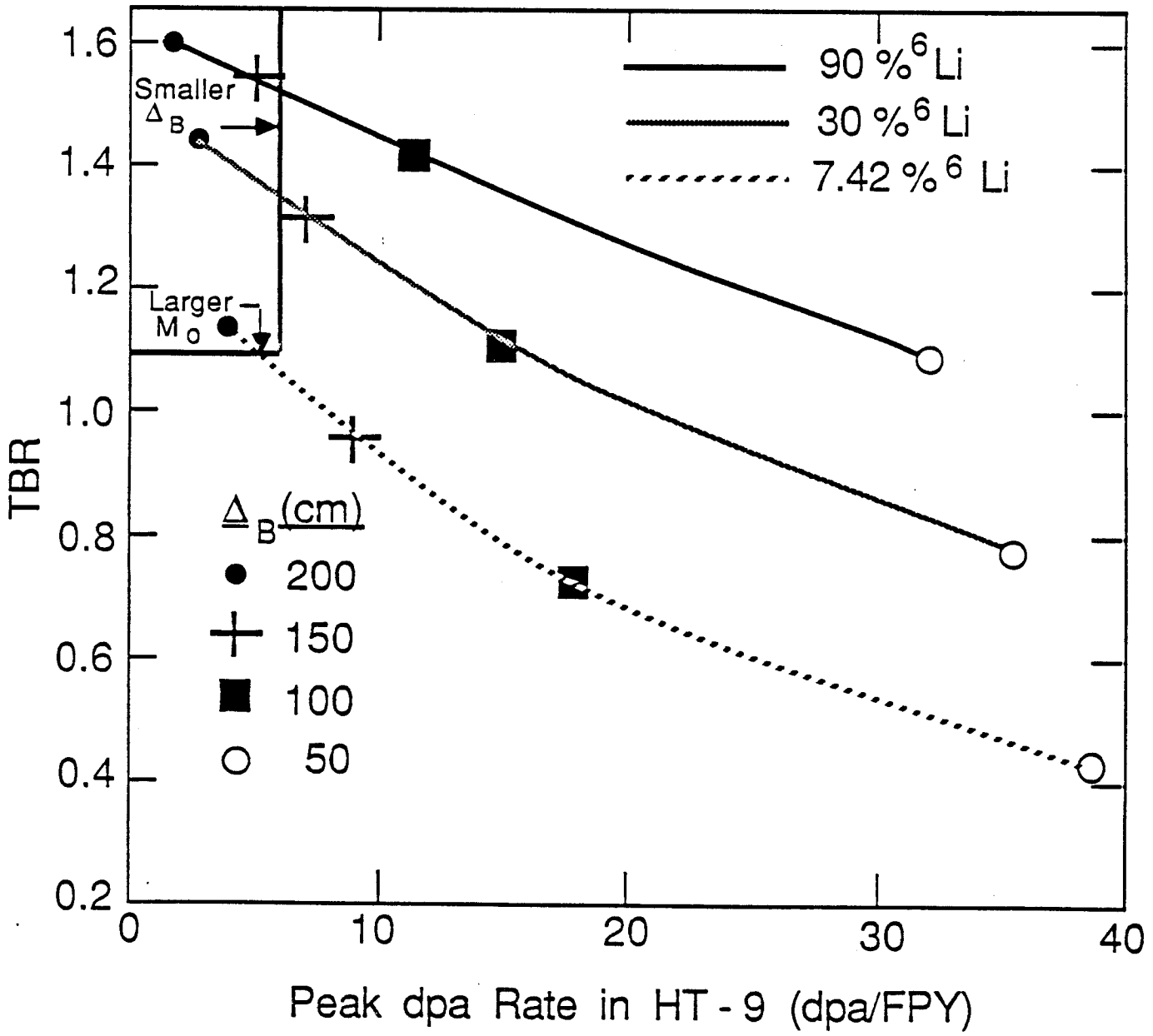

Figure 6-1. TBR vs. Damage Rate for the Blanket Design Options Considered.

Table 6-2 gives the nuclear parameters for the different options that satisfy the design requirements. While all options allow the reflector to be a lifetime component different values of TBR and M are obtained. The high enrichment option yields the thinnest blanket but the energy multiplication is relatively low and excessive tritium breeding is obtained. The largest M is obtained using natural lithium in the $Li_{17}Pb_{83}$ blanket but the channel length should be at least 5.4 m. The choice between these options should be based on economic and environmental considerations in addition to technical limitations for interfacing components such as the limitation on channel length. If the reflector is not required to be a lifetime component one can design the blanket to be as thin as 50 cm with 90% ^6Li enrichment yielding a channel length of 4 m. In this case the reflector has to be replaced four times during the reactor life. The impact on the cost and reactor availability needs to be assessed.

Progress on Mechanical Response of First Wall INPORTs

All theoretical aspects of the analysis of the dynamic response of flexible INPORTs have been completed. The sequential impulse code has essentially been fully developed and applied to a number of cases in which the predominant dynamic effects are linear. Early versions of this used the fundamental mode to characterize the response. The current form incorporates the first fifteen harmonics. A typical displacement-time history is shown in Fig. 6-2. Such response curves have been presented at recent progress meetings. In addition, linear parametric results have been determined for maximum steady-state displacement as a function of the impressed repetition rate. Conceptually this involves fixing the system parameters (tension, flow rate, mass per length, damping, elastic modulus, etc.) and running the displacement code for a range of repetition rates, i.e., simulating steady state response as the rep rate is continuously varied. This is computationally intensive but such information is important for identifying resonant peaks in the response. Figure 6-3 is used to show these characteristics. It should be re-emphasized that Fig. 6-2 would contribute one data point for a curve such as Fig. 6-3.

When nonlinear dynamic effects cannot be neglected, the amplitude-repetition rate curves corresponding to Fig. 6-3 are much more complicated. The distinguishing characteristics are discontinuities or jumps between different branches of the curves. Because of these difficulties, determining results for a wide range of variables is not practical. Efforts are being made to narrow the range of physical terms, particularly those influencing nonlinear contributions. When this is established, computations for the limited parameter values will be carried out to support a credible first wall-blanket design.

Table 6-2.
LIBRA Blanket Design Options Satisfying TBR and Damage Requirements (no reflector replacement)

% ^{6}Li	Δ_B (cm)	TBR	M_o	dpa/FPY	He appm/FPY
90	135	1.5	1.183	6.6	3.5
30	153	1.32	1.215	6.6	2.0
7.42	190	1.1	1.248	4.4	0.8

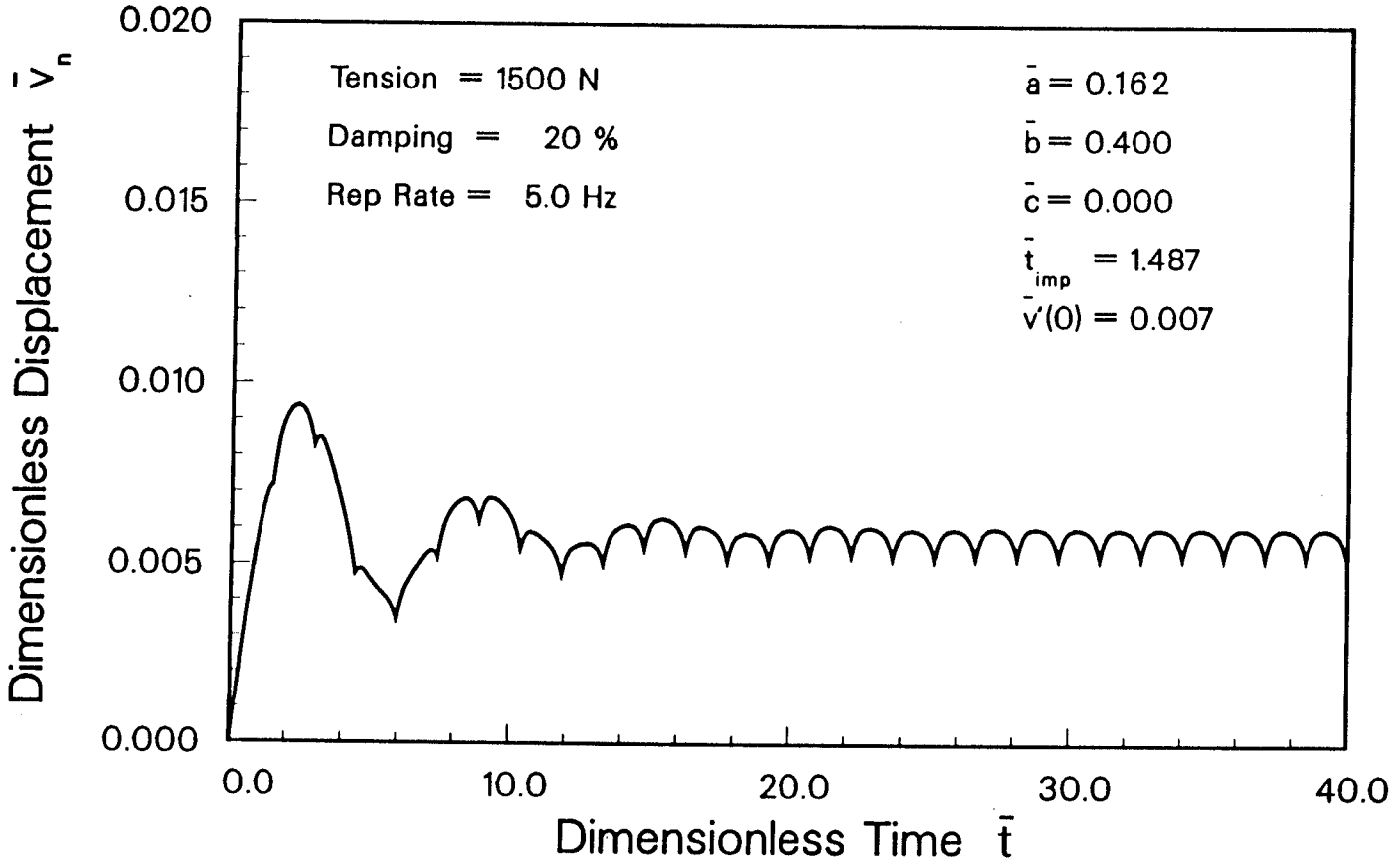

Figure 6-2. INPORT Midspan Displacement History.

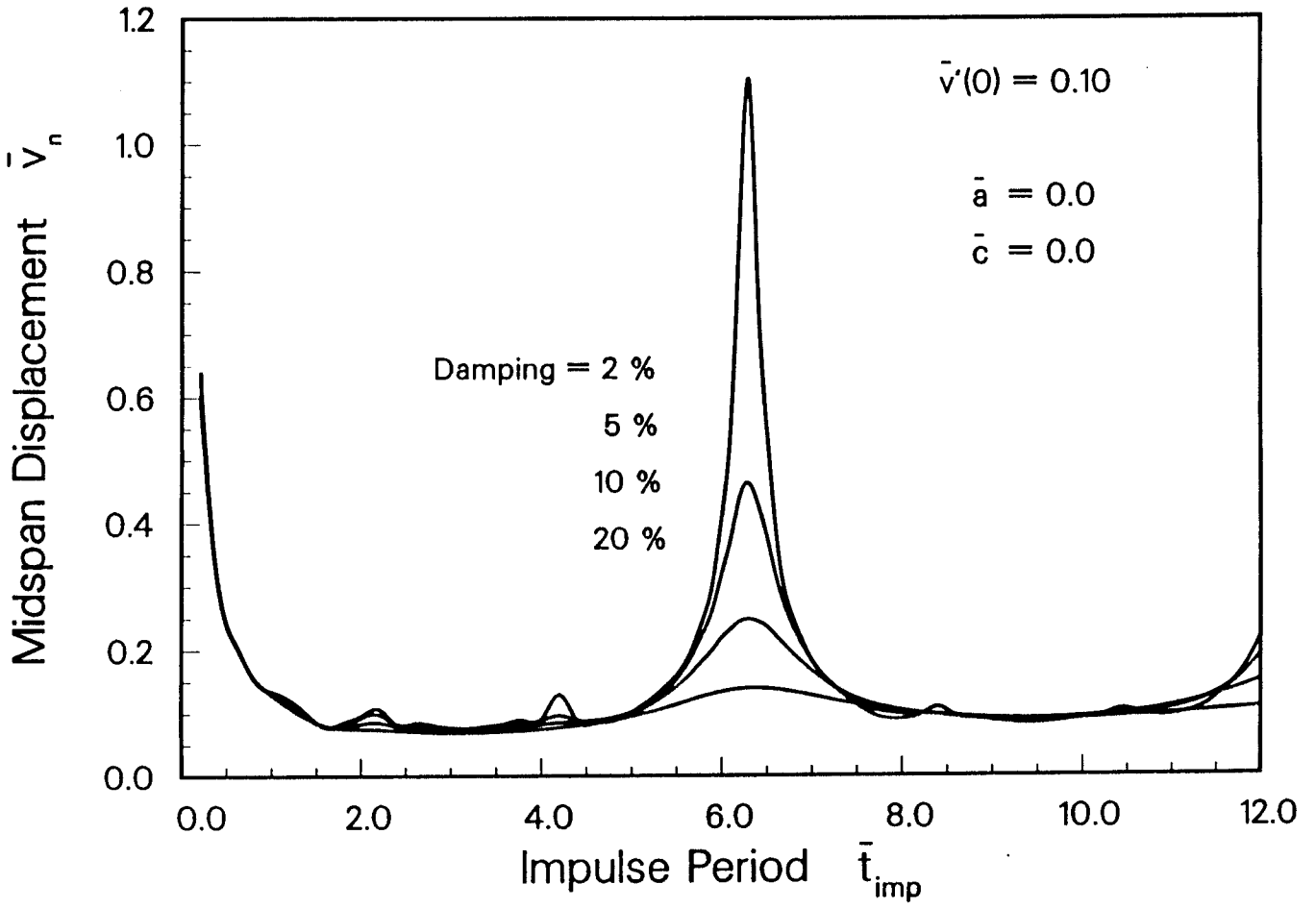

Figure 6-3. Planar Midspan Amplitude-Frequency Response.

7. TRITIUM FUELING, BREEDING AND RETENTION

During full-power operation, frozen fuel pellets may contain 1.28 mg of deuterium and 1.92 mg of tritium and are delivered at the rate of 3 Hz to the reactor. Because the fuel burnup is ~ 30%, nearly 1.73 mg/s of tritium must be produced in the LiPb liquid alloy in order to replenish the fuel supply. This breeder alloy also provides the heat transfer coolant for the INPORT tubes inside the reactor cavity. This sensible heat is transferred to a helium coolant circuit by means of a heat exchanger in the bottom pool of the reactor. Tritium removal is accomplished from both the heat transfer fluid circuits, as shown in Fig. 7-1, so that the tritium vapor pressure in the liquid alloy is $< 1.3 \times 10^{-2}$ Pa and the tritium permeation through the steam generator is < 100 Ci/d.

The amounts and locations of retained tritium inventories within the power plant are important quantities which must be determined in order to assess the safety of the facility during off-normal events. The reactor site will probably consist of a reactor hall containing the reactor cavity and ancillary equipment, and a separate fuel processing/fabrication facility. The quantities of tritium in each of these facilities have been estimated, see Table 7-1.

In the reactor hall, a supply of fuel pellets sufficient for one hour of fueling (~ 21 g of tritium) will be retained in a heavy, vacuum enclosed, cryogenic chamber. In the event that this chamber becomes overheated, the DT gases will be vented to an evacuated vessel of sufficient volume to store these gases below atmospheric pressure. The tritium within the reactor cavity is principally contained in the liquid breeder and SiC fibers of the INPORT tubes which are in contact with the liquid breeder. The concentration of tritium in the liquid breeder is controlled by the rate at which the liquid alloy is diverted to the Tritium Removal System (TRS) and the efficiency of the TRS. Because the tritium partial pressure is much larger for solutions of tritium dissolved in the liquid LiPb alloys as compared to liquid lithium, previous studies have shown that an efficient TRS method can be obtained by the vacuum degassing of a spray formed from the LiPb alloy. The spray droplets, 1 mm radius, fall approximately 10 m by gravity. For a reasonably sized vacuum pumping system, a tritium partial pressure of 1.3×10^{-2} Pa can be maintained for the LiPb alloy. When this tritium partial pressure is combined with the experimental derived Sievert's constant for this alloy, 1.2×10^{-3} wppm/$Pa^{1/2}$, it is calculated that the inventory for the entire liquid breeder system (540 metric tonnes) is < 0.1 g of tritium.

Table 7-1.

Tritium Inventory

Location	Tritium, g	
In Reactor Hall		
Fuel Supply (1 hr)	21	
Reactor Cavity		
SiC (INPORT tubes)	10	
LiPb (liquid alloy)	0.1	
		31
In Fuel Fabrication Building		
Fuel Processing	20	
Pellet Fabrication	60	
Pellet Storage (1 day)	500	
		580
TOTAL		611

Figure 7-1.

TRITIUM REMOVAL SYSTEMS IN LIQUID BREEDER AND HELIUM COOLANT CIRCUITS

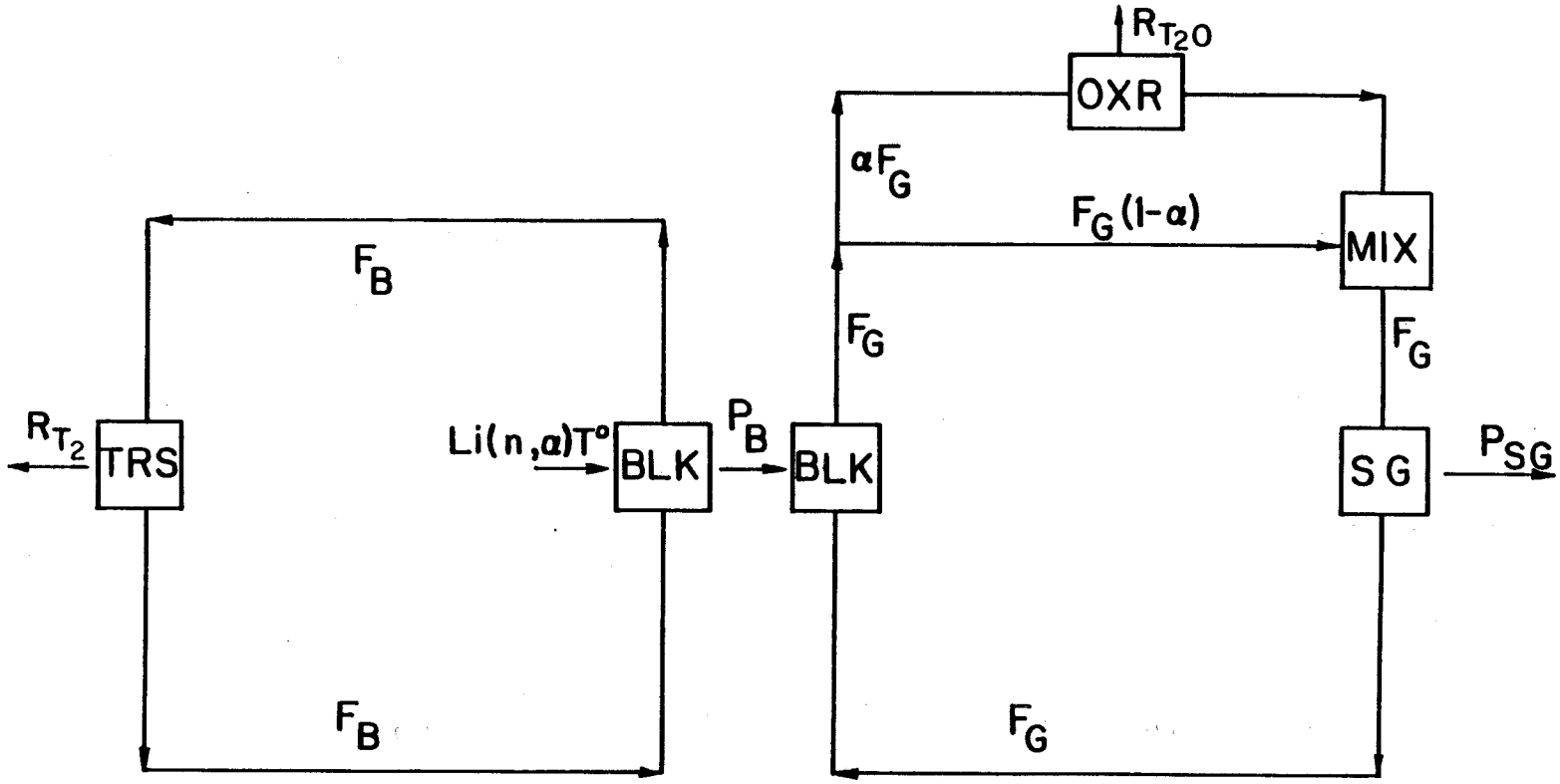

LIQUID BREEDER CIRCUIT **HELIUM COOLANT CIRCUIT**

F_B = flow rate of breeder
F_G = flow rate of coolant gas
α = fraction of gas flow to OXR
TRS = Tritium Removal System for liquid breeder
OXR = Tritium Removal by Oxidation & Adsorption

T^o = rate of tritium breeding
P_B = tritium permeation rate to the coolant gas
P_{SG} = tritium permeation rate to the steam circuit
BLK = Breeder liquid to helium coolant heat exchanger
SG = Steam Generator
R_{T_2} = rate of tritium removal

The solubility of the hydrogen isotopes dissolved in the SiC fibers of the INPORT tubes as a function of the concentration of hydrogen in the LiPb breeder alloy has not been determined. The solubility of gaseous deuterium in high purity α and βSiC powders has been determined as a function of D_2 pressure. Although the gross crystal structure of the fibers resembles βSiC, their chemical constituents are different. The fibers are formed from extruded methylcarbosilane polymers which are initially oxidized at 200°C and latter pyrolyzed at 1200°C to form SiC fibers. These fibers contain excess carbon and oxygen. The incorporation of oxygen in the fibers is believed to greatly reduce the rate and inventory of dissolved hydrogen as compared to the βSiC powders; consequently, the proposed solubility of tritium in the fibers was reduced to be more closely aligned with αSiC powders, which absorb less hydrogen, and extrapolated to the temperature (500°C) of the fibers in the INPORT tubes. Based upon these estimates, the tritium inventory in the fibers, 580 kg SiC, of the INPORT tubes is ~ 10 g.

In a separate Fuel Processing Building the tritium will be recovered from the TRS and the reactor exhaust gases. Tritium with additional D_2 will be fabricated to form the frozen fuel pellets. The quantity of T_2 and D_2 in the reactor cavity exhaust stream will probably be small because most of the unburned fuel should form LiT(D) and remain in the reactor. The tritium and deuterium recovered from the TRS will be chemically purified from trace impurities following procedures for the formation of high purity H_2. Finally the hydrogen isotopes will be separated by cryogenic distillation. If polarized fuel is needed, only the molecular species, DT, can be utilized. Approximately 20 g of tritium will reside in the fuel purification systems.

The technology for mass production of frozen DT fuel pellets does not exist at this time but is being actively developed. Currently, spherical shells of glass or polymers are filled by the permeation of pressurized DT through the shell walls at elevated temperatures. Recently, lithium metal foils, 25 μm thick, have been prepared and thinner walls may be possible. We suggest, therefore, that hemispherical Li shells could be sealed in a pressure chamber containing DT at ~ 45 MPa so that they would contain the required amount of frozen DT at cryogenic temperatures. These Li spheres would then be enclosed in preformed Pb hemispheres and sealed. If polarized fuel is desired it would be necessary to place the filled fuel pellets in a high magnetic field which requires many hours to polarize a significant fraction of the fuel. By the use of advanced nuclear magnetic resonance techniques which are presently being studied, it may be possible to

reduce this time to only several hours. We estimate, therefore, that it would take 3 hr to prepare a one hour fuel supply so that the fuel fabrication inventory would be ~ 60 g of tritium.

In case the fuel fabrication facility was not able to operate, some inventory of fabricated fuel pellets must be on-hand or else the power reactor would be shut down. The recent Heavy Ion Beam Reactor Study suggested that a one-day's supply of fuel should be adequate for this purpose; consequently, 500 g of tritium would be contained in this pellet inventory. A one day hold time for polarized fuel is also suggested because the fuel rapidly becomes depolarized by the beta particles from the decay of tritium. This large batch of fabricated fuel pellets would be securely protected in a cryogenic vault. In case of a failure of the cryogenic system the DT gases would vent to evacuated tanks kept below atmospheric pressure.

8. SUMMARY

The preconceptual design of the LIBRA reactor has progressed well in 1987. Selected parts of the design to be done by Fusion Power Associates are briefly summarized in this report. Integration with the target, driver, diodes, balance of plant, and cost assessment will be completed in 1988.